ELSEVIER

Polymer 42 (2001) 8447–8460

polymer

www.elsevier.nl/locate/polymer

Melting behavior and equilibrium melting temperatures of syndiotactic polystyrene in α and β crystalline forms

C. Wang*, Y.-C. Hsu, C.-F. Lo

Department of Chemical Engineering, National Cheng Kung University, 701-01 Tainan, Taiwan, ROC

Received 13 December 2000; received in revised form 26 February 2001; accepted 14 March 2001

Abstract

Syndiotactic polystyrene (sPS) specimens with neat α- and β-form crystals were prepared by using press molding under different conditions. The crystal form of the as-molded specimens was verified using wide angle X-ray diffraction and Fourier transform infrared spectroscopy techniques. Isothermal crystallization of α- and β-form sPS was conducted at various temperatures T_c and periods t_c. The corresponding melting enthalpies and temperatures upon subsequent heating were determined using differential scanning calorimetry (DSC). At given T_cs, the melting temperatures at zero crystallinity were deduced and used for the determination of equilibrium melting temperature, T_m^0, for both crystal forms. Based on the linear Hoffman–Weeks (HW) plots, the values of T_m^0 for α- and β-form sPS are obtained to be 281 and 291°C, respectively. The corresponding thickening coefficients are ca. 1.89 and 1.58, which seem unexpectedly high in consideration of the limited growth of lamellae at the early stage of crystallization. When a recently developed *MX* plot that is based on a non-linear HW approach is applied, reasonable thickening coefficients but much larger T_m^0 values are derived; being 294 and 320°C for α- and β-form sPS. On the basis of Avrami plot, the β-form crystals show three-dimensional growth, which is different from that for α-form crystals showing one-dimensional growth. For specimens with mixed α/β-crystals, the details of crystal development during the isothermal crystallization at 240°C is provided to account for the observation of the triple melting peaks which is normally detected by DSC heating scan.

Keywords: Syndiotactic polystyrene; Melting; Crystallization

1. Introduction

Syndiotactic polystyrene (sPS) is a new material with many unique properties, such as low dielectric constants, good chemical resistance and high melting temperatures, which makes it very attractive for use as a high-quality engineering thermoplastic. It is a semicrystalline polymer with a glass transition at around 95°C and an apparent crystalline melting point around 270°C. Depending on forming conditions, four types of crystalline structures can exist, denoted as α-, β-, γ- and δ-form, to develop the polymorphic behavior of sPS. Mechanical properties and chemical resistance of sPS specimens are associated with crystalline structure as well as crystallinity and their morphology. Development of the planar zigzag backbone is found in the α and β crystalline forms with hexagonal and orthorhombic symmetries, respectively [1,2]. Both α- and β-form crystals are obtained from melt crystallization but the β-form is more stable than the α one. Due to the difference in thermal stability and memory effect, the transformation of the less stable α-form into the β-form upon melting at high temperatures (above 300°C) and long holding time have been observed [3]. In contrast, helical backbone structure is usually detected in the γ and δ crystalline forms with monoclinic symmetry which is associated with solvent crystallization [4–6]. There are many articles to discuss the characteristics of crystalline structures and possible crystal transform using wide angle X-ray diffraction (WAXD) [3,4,7] and Fourier transform infrared spectroscopy (FTIR) [8,9].

The determination of the equilibrium melting temperature (T_m^0) of sPS is of importance since crystallization kinetics mainly depend on the amount of undercooling, ΔT ($= T_m^0 - T_c$, and T_c is the crystallization temperature). Linear Hoffman–Weeks (HW) plot is of wide utility for the T_m^0 determination of crystallizable polymers although the assumptions based are not strictly true, as we shall see in the following discussion. In this approach, the measured melting temperatures, T_ms, of specimens crystallized at T_cs are plotted against T_cs and a linear extrapolation is

* Corresponding author. Tel.: +886-6-2378422/2757575, ext. 62645; fax: +886-6-2344496.

E-mail address: chiwang@mail.ncku.edu.tw (C. Wang).

0032-3861/01/$ - see front matter
PII: S0032-3861(01)00360-3

conducted to the line $T_m = T_c$ where the intercept gives T_m^0. There are only few articles in the literature to discuss the equilibrium melting temperature of sPS with respect to its crystalline form. By measurements of the loss of the birefringence patterns, Cimmino et al. [10] obtained the melting temperatures of sPS ($M_w = 710$ kg/mol) at different T_cs. The value of T_m^0 was determined to be 275°C but no information regarding the crystal form, either α- or β-form was provided. Arnauts et al. [11] have conducted the differential scanning calorimetry (DSC) measurements to determine the T_m^0 value of sPS ($M_w = 79$ kg/mol) with β′-form crystals. Two melting peaks were observed when crystallization was carried out at low T_c (225–240°C). At higher T_c (240–250°C), only one melting peak was observed instead. Using the results at high T_c, an extrapolated T_m^0 value of 285.5°C was obtained according to the classical HW plot. Woo and Wu [12] found three melting peaks (three T_ms) on heating sPS specimens ($M_w = 241$ kg/mol) crystallized at low temperatures; suggesting that the lowest T_m is attributed to β-crystals, the intermediate T_m is associated with α-crystals and the highest T_m is relevant to the less stable β′-crystals. Based on the HW plots of the lowest and intermediate T_m, they obtained the same T_m^0 value of 285°C for β- and α-form crystals from. An even higher melting temperature of sPS, 291.5°C, can be obtained by Gvozdic et al. [13] using an extremely careful annealing method on sPS specimens with $M_w = 360$ kg/mol.

It should be noted that HW plot is based on an important assumption that the thickening coefficient for lamellae, $\gamma = l/l^*$ where l^* and l are the thickness of the virgin lamellae and that at the time of measuring respectively, is independent of crystallization temperature and time(t_c). The validity of this assumption is seldom verified so that the deduced T_m^0 values available in the literature may differ significantly from each other. From the thermodynamic stability consideration, the virgin lamellar thickness is mainly dependent on the degree of undercooling ΔT and thus T_c. Using real-time small angle X-ray scattering techniques, Albrecht and Strobl [14] were able to follow the growth of lamellar thickness of polyethylene starting at the very beginning of crystallization. They found a logarithmic time dependence of lamellar thickness at a given T_c. In other words, the lamellar thickness, l, depends not only on T_c but also on t_c due to the thickening effect. Thus, it is expected that values of γ are functions of both T_c and t_c that may contradict the assumptions of HW plot even though a linear relation between T_m and T_c is frequently obtained. In order to acquire the meaningful T_m^0 values from HW plots, the melting temperature at zero crystallinity is preferred to represent the T_m of the virgin lamellae of which the lamellar thickening effect is greatly limited.

Another difficulty encountered in the determination of T_m^0 of sPS is its polymorphic characters, leading to multiple melting peaks during DSC heating scans that further complicates the situation. It is reasonable to expect that the T_m^0 values of α- and β-form sPS are different from each other due to the differences in crystal lattice and molecular arrangement in the lattice. Indeed, owing to a denser packing in the orthorhombic lattice, β-form sPS has a larger crystal density of 1.067 g/cm^3, compared to that for α-form sPS in the hexagonal lattice, 1.033 g/cm^3 [15]. The T_m^0 difference resulting from polymorphic characters has been demonstrated in isotactic polypropylene, which possesses crystals with monoclinic and hexagonal symmetry, leading to the T_m^0 values of 208°C for the former and 184°C for the latter [16]. Although much attention has been paid to the studies of the relation between the crystal forms and melting behavior, the assignments of individual melting peak is not an easy task and still uncertain yet. In general, three melting peaks [17] are observed at T_c smaller than 247°C. The lowest melting peak temperature, T_{m1}, and its corresponding endothermic enthalpy both increase with T_c. The intermediate melting peak, T_{m2}, is also shifted to a higher temperature when specimens are crystallized at higher T_c. However, the highest melting peak temperature, T_{m3}, is irrelevant with T_c. At $T_c = 249$°C, an evident melting peak with a right shoulder is observed. Further increase in T_c leads to a single melting peak. Using WAXD and DSC, Hong et al. [18] studied the isothermal crystallization of sPS with mixed α- and β-forms. The population of α-form crystals decreases at high T_c. Eventually, the content of α-form is zero at T_c higher than 260°C when an extrapolation is made in Fig. 7 of Ref. [18]. In other words, only the nuclei for the β-form crystals can develop and grow at T_c higher than 260°C. In addition, they concluded similar assignments of T_m to crystal forms with that reported by Woo and Wu [12] except the highest T_m which is considered to attribute to the melting of sPS crystals recrystallized during DSC heating.

Melt recrystallization of β-form crystals is evidenced by two facts [17,19]. The first is the presence of a small exotherm between T_{m1} (due to melting of β-form crystals) and T_{m2} (due to melting of α-form crystals) during DSC heating under appropriate conditions. The second is the gradual increase of transmitted light under the observation using an optical microscope with cross polars when temperature is maintained constant between T_{m1} and T_{m2} after partial melting the sPS crystals [19]. The event of recrystallization during melting further complicates the determination of T_m of the individual crystals, especially that for α-form since the T_{m2} value is now dependent on the composite curve consisting of the recrystallization exotherm and the genuine melting endotherm of α-form crystals. This might result in an erroneous determination of T_m^0 for α-form crystals provided that peak separation (two melting peaks and one recrystallization 'valley') has not been carefully conducted to draw the correct T_{m2} for the HW plot.

To estimate the accurate T_m^0 values for α- and β-form sPS, the crystallization conditions have to been controlled with great care to exclude any possible crystal transformation and recrystallization during DSC heating scans. One way to reach this goal is to prepare neat α- and β-form

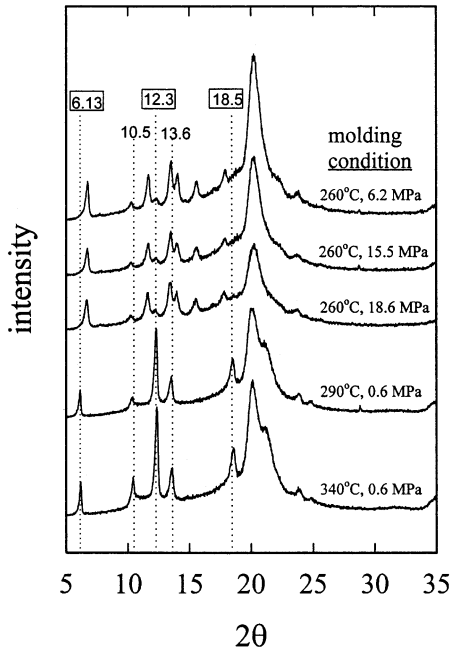

Fig. 1. WAXD patterns for sPS specimens pressed at different molding conditions (the dotted lines denote the positions of characteristic diffraction peaks for β′-form).

specimens individually and make them crystallize at relatively high T_c where a single melting peak is detected during the subsequent heating. In this publication, an attempt is made to quantitatively characterize melting behavior of α- and β-form sPS that are prepared from press-molding. The equilibrium melting temperatures are deduced and thermodynamic parameters are reported as well.

2. Experimental

sPS pellets with $M_w = 200$ kg/mol was kindly provided by Dow Chemicals. Different conditions for press molding were used to prepare sPS specimens with neat α-form (and β-form) crystals exclusively for the further microstructure characterization. Based on our preliminary studies [17] and the suggestions given in a previous article [3], less stable α-form specimens can be obtained when thermodynamic equilibrium melting of original pellets is hard to achieve. To prepare specimens with neat α-form crystals, the sPS pellets were placed in a disk-shaped mold (diameter = 17 mm and thickness = 1.2 mm) and molded at 260°C and high pressures (6.2–18.6 MPa) for 3 min, followed by ambient cooling under the set pressures. On the other hand, stable β-form specimens were prepared under the conditions of high temperatures and low pressures (e.g. 290°C and 0.6 MPa). The pellets were first melted at high temperatures (290–340°C) and 0.6 MPa for 10 min and then cooled slowly at atmosphere pressure. The as-molded specimens were characterized using a 18 kW rotating anode X-ray generator (Cu target, Rigaku) operated at 40 kV and 100 mA with a 2θ scan rate of 4°/min. To verify the crystal forms, attenuated total reflection (ATR) technique was also applied using a Perkin–Elmer 1725X apparatus to obtain the FTIR spectrums of the as-molded specimens. For each measurement, 64 scans were conducted with a resolution of 2 cm^{-1}.

The crystallization kinetics and melting behavior were investigated with a Perkin–Elmer DSC-7 differential scanning calorimeter equipped with an intra-cooler. The specimens for DSC measurements were obtained by slicing the center portion of the molded disks. Before measurements, temperature calibration was conducted using zinc (419.5°C) and indium (156.6°C). For neat β-form sPS, the specimens were first heated to 300°C for 10 min in a nitrogen atmosphere. Rapid cooling was carried out to the desired temperature, T_c, for isothermal crystallization. After the specimens were crystallized for a specified time, t_c, heating scan was conducted directly from T_c to 300°C at 10°C/min and the melting endotherm was recorded. For a given T_c and t_c, the corresponding melting temperature and the enthalpy were determined from the peak position and area of the recorded endotherm. For neat α-form sPS specimens, similar crystallization conditions were also applied except that different holding temperature and period for melting were used prior to crystallization. Cautions had been taken to avoid the possible crystal transformation from less stable α-form crystals to more stable β-form ones during the heat treatments [3]. To preserve α-form crystals, the neat α-form specimens were held at 280°C for 3 min prior to crystallization, instead of that (300°C for 10 min) used for neat β-form sPS. The temperature range for crystallization studied was 249–269°C for α-form specimens and 249–267°C for β-form ones where a single melting peak was always observed during heating scans to exclude the occurrence of complicated multiple melting peaks.

3. Results and discussion

3.1. Characterization of α- and β-form sPS

Fig. 1 shows WAXD profiles for specimens press molded under different conditions. The appearance of characteristic diffraction peaks at $2\theta = 6.72$ and 11.7° is attributed the presence of α-form crystals [3]. On the other hand, β-form crystals show the characteristic peak positions at $2\theta =$ 6.13 and 12.3° [1]. As shown in Fig. 1, it is obvious that specimens molded at high temperatures and low pressures (either at 290°C and 0.6 MPa or 340°C and 0.6 MPa) show only β-form WAXD patterns and are considered as neat β-form sPS. Indeed, it can be further characterized as β′-form sPS for the less order structure according to the crystal lattice specification (the dotted lines in Fig. 1 denote the diffraction angles associated with β′-form crystals, $2\theta =$ 6.13, 10.5, 12.3, 13.6 and 18.5°). Neat α-form sPS is obtained when specimens are molded at low temperatures and high pressures where thermodynamic equilibrium of

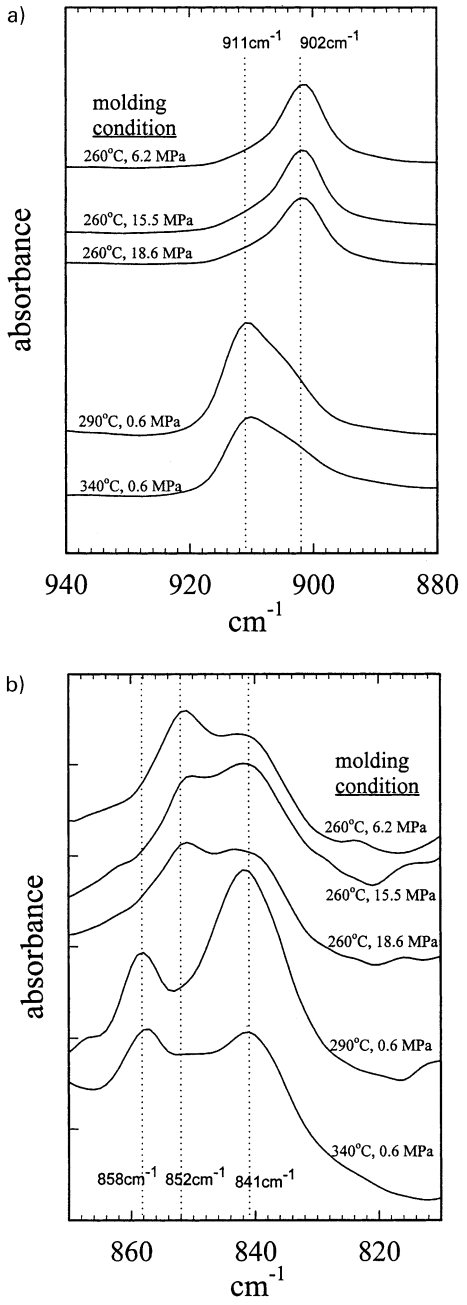

Fig. 2. FTIR patterns for sPS pressed at different molding conditions (a) for wavenumbers from 880 to 940 cm^{-1}, where 902 and 911 cm^{-1} are attributed to that for α- and β-forms, respectively, (b) for wavenumbers from 810 to 870 cm^{-1}, where 852 and 858 cm^{-1} are attributed to that for α- and β-forms, respectively and 841 cm^{-1} is associated with amorphous phase.

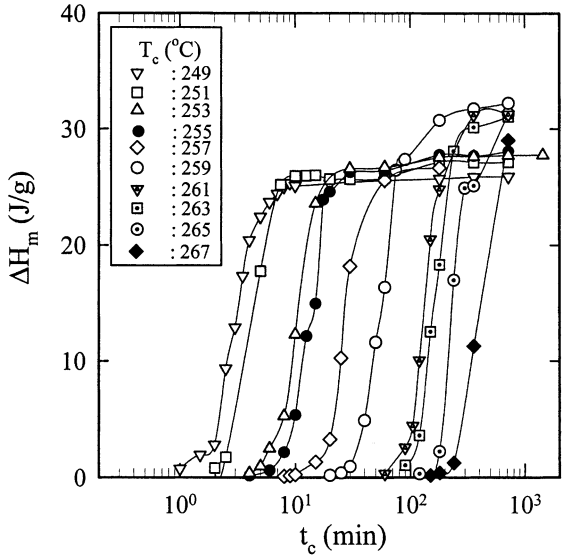

Fig. 3. Melting enthalpies ΔH_m of β-form specimens crystallized at various times t_c and temperatures T_c (heating scans starting from T_c with a rate of 10°C/min).

melting is not easy to reach. Although a rather small diffraction peak at $2\theta = 12.3°$ associated with β-form crystals is detected, the specimens molded at 260°C and 15.5 MPa are taken as neat α-form sPS. Similarly, it is further characterized to be α″-form sPS for its relative ordered structure, giving rise to the appearance of diffraction peaks at $2\theta =$ 6.72, 10.3, 11.7, 13.5, 14.0 and 15.6°. It should be noted what we observed here is significantly different from that reported by Sun et al. [15], reporting that α-crystals are favored for specimens annealed at 260°C and atmospheric pressures, but β-crystals are developed when annealed at 260°C and high pressures.

To further characterize the relative amount of α- and β-form crystals in the sPS specimens, FTIR is also a feasible technique to carry out. It has been pointed out that three absorbance peaks are detected in the wavenumber range of 880–940 cm^{-1}; the peak at 902 cm^{-1} is associated with α-form crystals, 911 cm^{-1} is relevant to β-form crystals and 906 cm^{-1} is attributed to the presence of amorphous sPS [8]. Thus, the relative amount of α/β-crystals can be estimated from the height ratio of absorbance peaks at 902 to 911 cm^{-1} from the FTIR spectrum. Fig. 2(a) shows the FTIR spectrums obtained in this region for specimens press molded under different conditions. It is interesting to note that a symmetric absorbance peak at 902 cm^{-1} is clearly detected when neat α-form crystals are developed; whereas an asymmetric peak is found at 911 cm^{-1} due to the evident presence of amorphous phase at 906 cm^{-1} when neat β-form crystals form. Another wavenumber region which is also useful to reveal the relative presence of sPS crystals is in the range of 810–870 cm^{-1}, as shown in Fig. 2(b). In this region, 841 cm^{-1} is assigned to the contribution from amorphous phase and the wavenumbers at 852 and 858 cm^{-1} correspond to the specific absorbance of α- and β-form crystals, respectively. In contrast to that in Fig. 2(a), the contribution from amorphous phase is more significant in this wavenumber range so that a spectral subtraction approach is suggested to obtain genuine results [20]. Nevertheless, a trend can still be drawn from the relative peak heights of 852 and 858 cm^{-1}, indicating the relative presence of α- and β-crystals. Based on Figs. 1 and 2, FTIR results are in good agreement with WAXD measurements, leading to a conclusion that press molding under

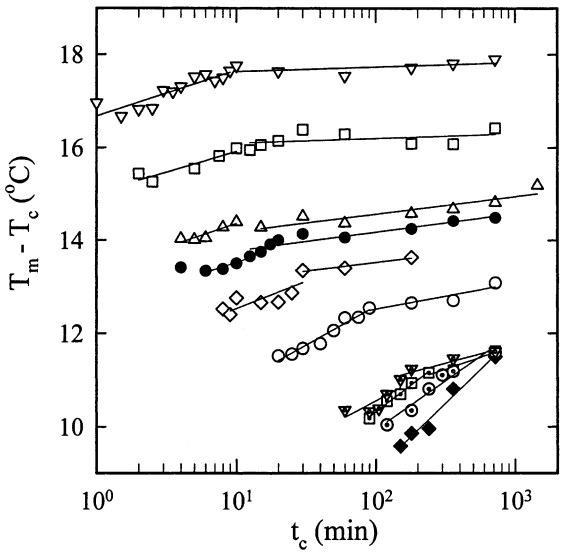

Fig. 4. Effect of crystallization time t_c on the melting temperature of β-form specimens crystallized at various T_c (symbol notations are the same as those used in Fig. 3).

conditions of high pressures and low temperatures favors the developments of α-form crystals due to its less stable nature.

3.2. Crystallization of neat β-form sPS

The DSC scans performed at 10°C/min on neat β′-form specimens crystallized at temperatures lower than 249°C show endotherms with a double peak shape. The presence of double-melting-peak behavior suggests the occurrence of either two different crystal thickness or crystal reorganization during heating scans which is beyond the scope of the present study. To simplify the situation, isothermal crystallization is set at high temperatures (249–267°C), where a single endothermic peak is always obtained. Fig. 3 shows the melting enthalpies of β-form sPS crystallized at given temperatures T_c as a function of crystallization time, t_c.

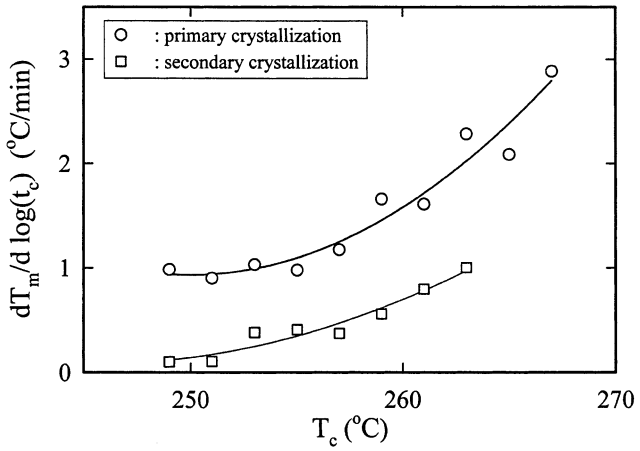

Fig. 5. Plots of $dT_m/d\log(t_c)$ versus T_c for β-form specimens.

Conventionally, the amount of melting enthalpy, ΔH_m, represents the level of crystallinity, provided that the heat of fusion for pure crystal, ΔH_f, is known. Since α- and β-crystals have different packing and lattice structures, the ΔH_f values for the individual crystals are expected to be different from each other. Using DSC, Gianotti and Valvassori [21] have studied the melting enthalpy of sPS crystals in the presence of diluents by a melting temperature depression approach. A deduced ΔH_f value of 82.4 J/g was obtained based on Flory's theory of polymer solutions, but no discussion regarding the crystal structure investigated was provided. In contrast, a relatively low value, $\Delta H_f = 53.2$ J/g, was reported by Paszlor et al. [22] using extrapolation from the plot of heat capacity change at T_g versus the observed heat of fusion. In consideration of the polymorphic nature of sPS (not only α- and β-crystals, but also crystals solvated with solvents or possible crystal transformation will take place, depending on the thermal history and environments), the discrepancy might be attributed to different crystals studied. To avoid the misleading interpretation due to the difficulty in obtaining 100% pure α- and β-crystals' ΔH_f, melting enthalpies were used thoroughly here instead of the degree of crystallinity to discuss the crystallization evolution.

During crystallization, two different processes are usually distinguished: the first is the primary crystallization where the superstructures form and grow to fill the available space [23]. It is followed by the secondary crystallization where crystal perfection within superstructures takes place. As shown in Fig. 3, after a certain induction time the ΔH_m increases abruptly to about 25 J/g during the process of primary crystallization. Afterwards, secondary crystallization takes place and a slight increase of ΔH_m is still observed. This trend holds valid for specimens crystallized at all given T_c, whereas the major distinction is the difference in induction time as shown in Fig. 3, revealing that it takes longer time for stable β-nuclei to form at a higher T_c. It is also intriguing to note that the final degree of crystallinity, i.e. ΔH_m at 720 min, is more or less the same in spite of 18°C difference in T_c (249–267°C). The final ΔH_m values are about 26–32 J/g obtained at $t_c = 720$ min. It is worthwhile to address that the β′-form crystalline structure is always preserved after isothermal crystallization for $t_c = 720$ min as revealed by WAXD techniques [17], involving no β to α crystal transformation taking place.

The corresponding T_ms, obtained from the position of the endothermic peak in the DSC scans performed at 10°C/min, are shown in Fig. 4 as a function of t_c. To measure the true T_m of the crystals formed at a given T_c and t_c, the subsequent heating scan has to be conducted with a rate sufficiently high to inhibit reorganization, yet avoid superheating. In consideration of the measured $T_m - T_c$ values shown in Fig. 4, the heating rate (10°C/min) seems appropriate to apply since a short melting period about 1–2 min is required to complete the melting. Evidently, different logarithmic time dependences of T_m should be separately applied for the primary

Table 1
The melting temperatures at zero crystallinity, T'_m, for α- and β-form sPS specimens crystallized at various crystallization temperatures, T_c

T_c (°C)	β-Form crystals T'_m (°C)	α-Form crystals T'_m (°C)
249	265.20	270.99
251	265.70	NA
253	267.03	271.57
255	268.13	270.36
257	269.46	271.65
259	270.52	271.32
261	271.36	272.54
263	273.00	271.89
265	275.04	272.72
267	276.58	273.08
269	NA	275.29

and secondary crystallization processes, as shown in Fig. 4. The calculated slopes, $dT_m/d\log(t_c)$ values, are shown in Fig. 5 as a function of T_c. The $dT_m/d\log(t_c)$ values for both primary and secondary crystallizations increase with increasing T_c. At a given T_c, moreover, a larger $dT_m/d\log(t_c)$ value is found for primary crystallization than that for secondary crystallization process. This is in contrast with the results for isotactic polypropylene which show a constant value of $dT_m/d\log(t_c)$ during the whole crystallization process [24]. The melting temperature is relevant to the lamellar thickness, according to the Gibbs–Thomson relation, which indicates that thicker lamellae will melt at higher temperatures. Therefore, lamellar thickening is evident for sPS, as indicated by the gradual shift of melting peaks to high temperatures, at all T_c when crystallization is carried out continuously for a long time. The rate of lamellar thickening ($dl/d\log(t_c)$), implicitly related with $dT_m/d\log(t_c)$, increases with increasing T_c. Present results further imply that lamellar thickening rate is larger during primary crystallization, compared with that for secondary crystallization. After deducing the induction time from

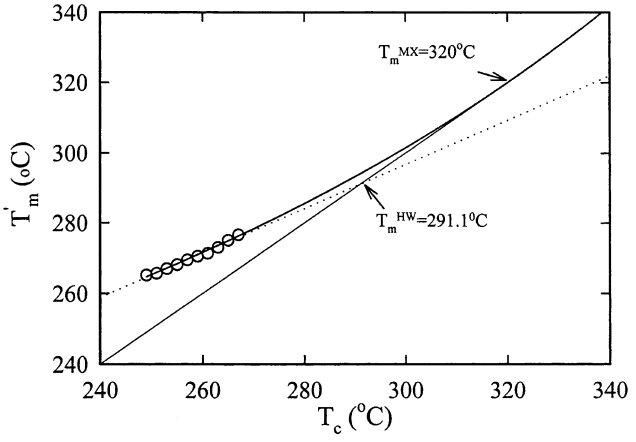

Fig. 6. Comparisons of the HW plot and the MX plot for β-form specimens, where T'_m is the melting temperature at zero crystallinity and T_c is the crystallization temperature (the dotted line and solid curve are constructed based on HW and *MX* plots, respectively).

Fig. 3, the melting temperatures at the zero crystallinity, T'_m, at each T_c were obtained by substituting the induction time into the linear relation of T_m–T_c versus $\log t_c$ in the primary crystallization, as proposed previously [24]. Variation of T'_m with T_c is tabulated in Table 1 and also shown in Fig. 6 where regression of the linear HW plot is also carried out and shown by the dotted line. The HW relation is expressed as follows:

$$T'_m = T^0_m(1 - 1/\gamma) + T_c/\gamma \quad (1)$$

According to Eq. (1), the thickening coefficient, γ, and the equilibrium melting temperature, T^0_m, for β-form sPS are determined to be 1.58 and 291°C, respectively. The derived T^0_m value in this manner is higher than those reported previously using the same approach (285.5°C by Aranuts et al. [11] and Woo et al. [12] and 278.6°C by Ho et al. [25]). Since high molecular weight of sPS were utilized in all cases, it was suggested that effects of defects due to the chain ends are excluded. The variation might be attributed to different degrees of syndiotacticity of sPS specimens used in this study and theirs. Another plausible reason is due to the thickening effect caused by the prolonged crystallization conducted in their measurements [11,12,25]. As pointed out by Mandelkern and co-workers [26], the experimentally measured T_m should be determined only at very low levels of crystallinity in accordance with HW theory. If one uses the T_m values at high levels of crystallinity (obtained at large t_c) instead, it will tend to decrease the linear slope and may result in an extrapolated T^0_m lower than the true one. For example, when the measured T_m of specimens crystallized for $t_c = 180$ min are plotted against T_c instead, values of γ and T^0_m are determined to be 1.63 and 290°C, respectively. For $t_c = 720$ min, on the other hand, the deduced γ and T^0_m values are 1.85 and 285.5°C which are close to Arnauts' results [11]. Thus, thickening effect plays a prominent role which may mislead the determination of T^0_m if experimentally measured T_m are obtained at high levels of crystallinity. To fulfill the underlying assumption of HW relation, melting temperatures at zero crystallinity are preferred to obtain a correct extrapolated T^0_m. Since extended time was adopted for crystallization in their studies [12,25], a pronounced and unpredictable crystal thickening effect might produce, leading the extrapolated T^0_m less reliable.

It should be noted that lamellar thickening must be greatly limited when measurement is carried out at the very early crystallization where extremely low crystallinity is obtained, leading to an estimated γ value of unity. However, the derived γ value ($= 1.58$) indicates a quick increase of 58% lamellar thickness even at the very early crystallization, i.e. conditions of zero crystallinity. As pointed out by Marand et al. [24,27], the linear HW plot is based on two major assumptions: the first is the T_c independence of thickening coefficient which may not be reasonable as mentioned previously, and the second is the

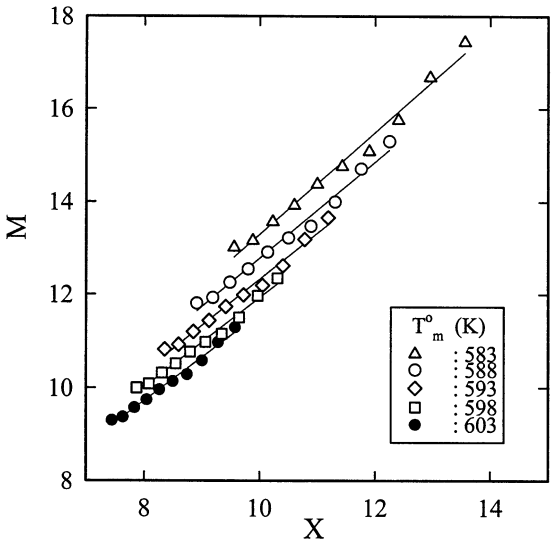

Fig. 7. *MX* plots to determine the thickening coefficient for β-form specimens at different specified equilibrium melting temperatures, T_m^0.

relation for virgin lamellar thickness given theoretically by $l^* = C_1/\Delta T$ which is different from the experimentally obtained relation: $l^* = C_1/\Delta T + C_2$ where C_1 and C_2 are constants. To compensate the discrepancy due to the second assumption, a linear *MX* plot approach has recently been proposed by Marand et al. [24,27] to obtain a more reliable and meaningful T_m^0 value. A simple relation for the reduced melting temperature, M, and the reduced crystallization temperature, X, has been derived as follows:

$$M = \gamma(X + a) \tag{2}$$

where $M = T_m^0/(T_m^0 - T_m')$, $X = T_m^0/(T_m^0 - T_c)$ and the parameter a is given by $C_2\Delta H_f/(2\sigma_e)$ with ΔH_f and σ_e being the heat of fusion of the crystal and the interfacial free energy of the basal face of crystals, respectively. One should note that Eqs. (1) and (2) both are based on the assumption that the

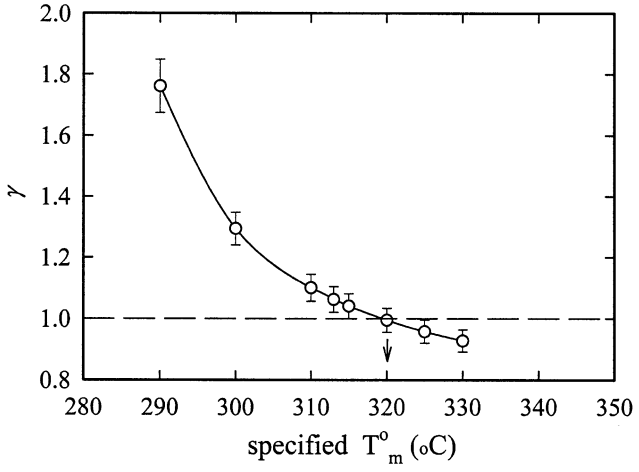

Fig. 8. Calculated thickening coefficients, γ, at different specified equilibrium melting temperatures, T_m^0, for β-form specimens (the genuine T_m^0 is determined at $\gamma = 1.0$ as pointed by the arrow).

interfacial free energy of basal faces for both virgin and mature crystals is the same. On the basis of Eq. (2), a plot of M versus X will give a constant slope of γ after a specified T_m^0 value is chosen. Thus, the genuine value of T_m^0 is obtained at the selected temperature where the calculated γ is equal to unity (i.e. no lamellar thickening taking place) since the melting temperature at zero crystallinity is applied. Fig. 7 shows the typical plots of M against X under the conditions that five specified T_m^0 are selected (583–603 K). The determined values of γ are further plotted against the specified T_m^0, as shown in Fig. 8. To intercept with the $\gamma = 1$ line, the genuine T_m^0 for the β-form sPS crystals is obtained to be ca. 320°C. The corresponding value of a is 2.38, leading to the C_2 value of 4.75 $(\sigma_e/\Delta H_f)$. After deducing the C_1 $(= 2\sigma_e T_m^0/\Delta H_f)$ value, the thickness of the virgin lamellae is then estimated by the following relation:

$$l^*(T_c) = (\sigma_e/\Delta H_f)_{\beta\text{-form}}\left[\frac{1186}{320 - T_c} + 4.75\right] \tag{3}$$

where $(\sigma_e/\Delta H_f)_{\beta\text{-form}}$ is a parameter for β-form crystals and T_c is in the unit of °C. The second term in the bracket is due to C_2 which is associated with the thickness increment δl^* to prevent the lamella melting at the temperature T_c where it is crystallized. It should be noted that the $\delta l^*/l^*$ fraction is about 0.22 at $T_c = 250$°C and a slightly lower value 0.17 at $T_c = 270$°C. Thus, the contribution of δl^* to the l^* cannot be neglected in the T_c range studied, fulfilling the assumption of *MX* plot and invalidating the application of linear HW plot. Significant contribution of δl^* to l^* has also been found on the studies of crystallization of PE [28,29], iPP [27] and iPS [28]. Moreover, the thickening coefficient as a function of t_c at a given T_c is expressed as follows:

$$\gamma(T_c, t_c) = \frac{M(t_c)}{X + 2.38} = \frac{593/(320 - T_m(t_c))}{593/(320 - T_c) + 2.38} \tag{4}$$

According to Eq. (4), the thickening coefficient increases with increasing T_c but the range of variation is not large, from $\gamma = 1.0$ at zero crystallinity to $\gamma = 1.07$ at most under the conditions of high T_c (267°C) and prolonged t_c (720 min). Besides the consequence of T_c and t_c dependence of the thickening coefficients, linear HW plot cannot readily applied to determine T_m^0 owing to a non-zero value of δl^* as well.

Recently, a similar approach has been also applied by Ho et al. [25] using the *MX* plot but a relatively lower T_m^0 value (306.9°C) has been obtained, compared to our present results (320°C). The discrepancy is attributed to two respects: Firstly, melting temperatures were measured in their experiments for neat β-crystal specimens crystallized in T_c range of 240–250°C where two melting peaks are evident, giving rise to a difficulty in peak assignments. Moreover, it has been noted that crystals developed at relatively low T_c will tend to thicken substantially during heating and the measured T_m will be quite a bit higher than the

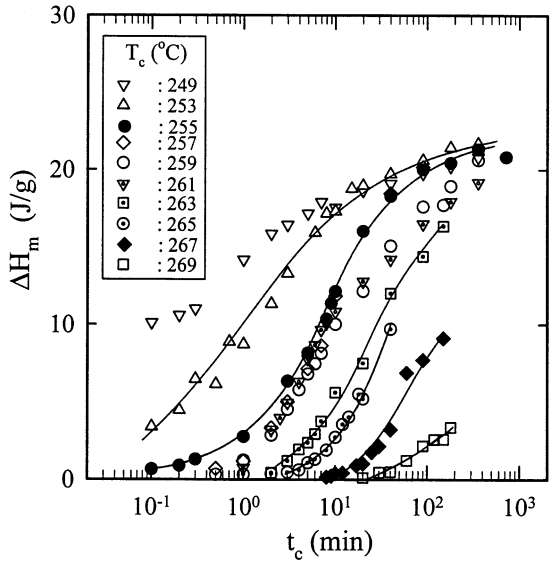

Fig. 9. Melting enthalpies ΔH_m of α-form specimens crystallized at various time t_c and temperature T_c (heating scans starting from T_c with a rate of 10°C/min).

true T_m. From the point of view of the HW plot (or the *MX* plot), this will tend to increase the γ value and may result in an extrapolated T_m^0 lower than the true value. Secondly, the crucial influence of t_c on the melting behavior (as shown in Fig. 4) has not been taken into account in their study so that the measured melting temperature of specimens crystallized at a given T_c may be higher than T_m' at zero crystallinity, as mentioned previously. It seems that utmost care has to be taken to derive a more reliable T_m^0 value from melting data. This is particularly important for sPS materials which possess complex polymorphic behavior and pronounced effects of t_c on the measured T_m as well.

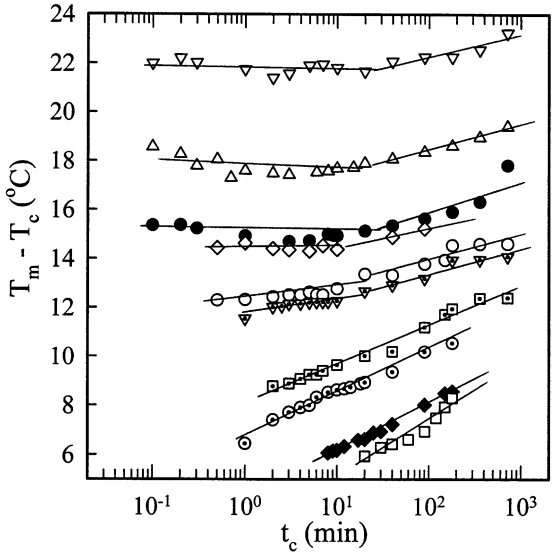

Fig. 10. Effect of crystallization time t_c on the melting temperature of α-form specimens crystallized at various T_c (symbol notations are the same as those used in Fig. 9).

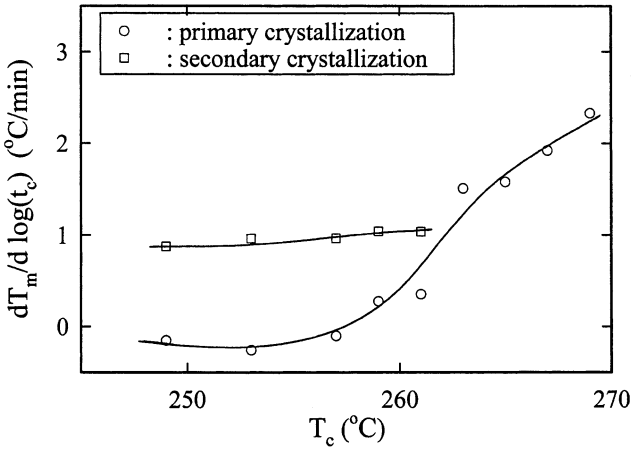

Fig. 11. Plots of $dT_m/d\log(t_c)$ versus T_c for α-form specimens.

3.3. Crystallization of neat α-form sPS

Isothermal crystallization of α″-form sPS was conducted in the T_c range of 249–269°C where a single endothermic peak was observed when a subsequent heating scan was performed at a rate of 10°C/min. Preservation of α″-crystals was verified using WAXD techniques. Melting enthalpies ΔH_m for α-form sPS crystallized at various T_c and t_c are given in Fig. 9, showing crystallization evolution different from that in Fig. 3 for β-form sPS. When crystallization takes place at temperatures lower than 255°C, stable α-nuclei are quickly developed owing to a very small induction time required. Indeed, when crystallized at $T_c = 253$°C the ΔH_m reaches a value of 3 J/g at $t_c = 0.1$ min, whereas it takes ca. 9.0 min for β-form sPS to develop the corresponding amount of ΔH_m, as shown in Fig. 3. Thus, the induction time for initial crystals to appear is significantly reduced for the α-form sPS, leading a better nucleating ability, compared to β-form sPS. When crystallized at T_c in the range from 255 to 261°C, superposition of the melting-enthalpy curves seems to occur, suggesting a similar kinetics for crystallization in this regime. The induction time is increased gradually at higher T_c, a phenomena similar with that for β-form sPS. However, the induction time is still much smaller than that for β-form crystals, for example it takes 10 min for α-form, compared to 110 min for β-form crystals at $T_c = 267$°C. In addition, the DSC endothermic peaks show a significant shift to high melting temperatures for specimens crystallized for a prolonged time so that the end of melting interval is beyond the holding temperature (280°C). Hence, accurate ΔH_m values of specimens crystallized for a long time in this T_c regime (263–269°C) are practically limited and are not shown in Fig. 9, whereas precise determination of melting temperature (determined from the peak temperatures) is certain, as shown in Fig. 10. At a given T_c, the t_c dependence of melting temperature exhibits different behavior from that for β-crystal specimens. In T_c range of 249–261°C, small negative values of $dT_m/d\log(t_c)$ are obtained for primary crystallization,

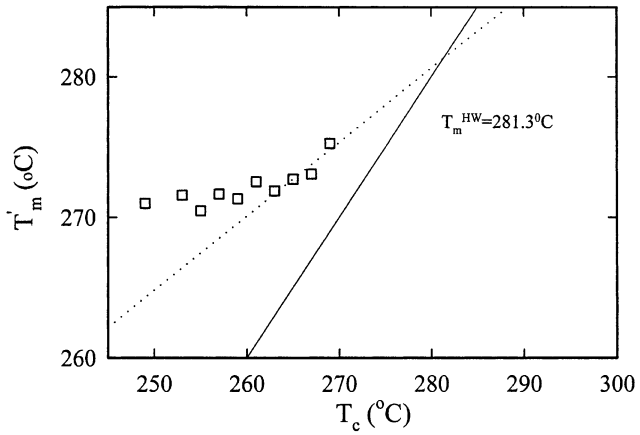

Fig. 12. HW plot for α-form specimens where T_m' is the melting temperature at zero crystallinity and T_c is the crystallization temperature; the dotted line is constructed for $T_c = 263–269$°C.

whereas the $dT_m/d\log(t_c)$ values for secondary crystallization is more or less constant (about ~1.0) but larger than that for primary crystallization, as shown in Fig. 11. It implies that once the virgin lamellae appear after induction, its thickness remains constant (or slightly decreased) until the available space for crystallization is occupied by the superstructures where secondary crystallization takes place and lamellar thickness gradually increases. On the other hand, an evident increase of T_m occurs during primary crystallization when specimens are crystallized at temperatures higher than 263°C (Fig. 10). The derived melting temperatures at zero crystallinity are plotted against the crystallization temperature as shown in Fig. 12. A constant T_m' value, ca. 271°C, is obtained when T_c is in the range of 249–261°C. When crystallized at higher T_c, the T_m' value is increased gradually, suggesting that the virgin lamellae developed in $T_c = 263–269$°C behave differently from

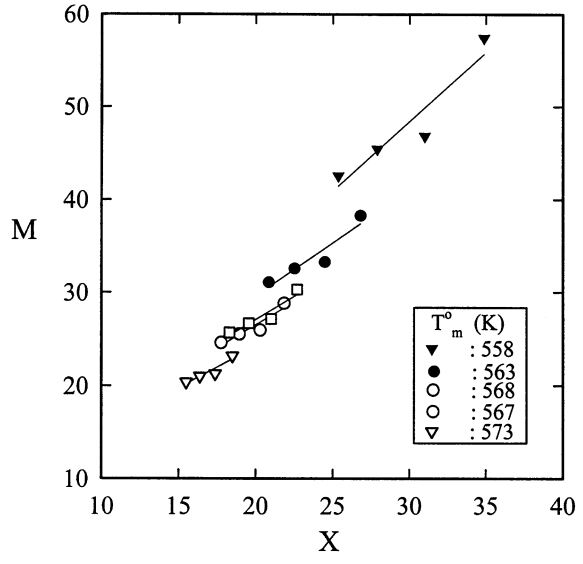

Fig. 13. *MX* plots to determine the thickening coefficient for α-form specimens at different specified equilibrium melting temperature T_m^0.

those at lower T_c. From the DSC and corresponding WAXD results, it has been pointed out previously [30] that a constant melting peak associated with α″-forms is normally observed at ca. 271°C and any presence of less ordered α′-form crystals will provide an additional melting peak at lower temperatures. Our present results also indicate that two separate melting peaks attributable to α′- and α″-forms, respectively can be observed when neat α-form crystals are crystallized at T_c lower than 249°C (as shown in Fig. 20(a) and discussed later). The position of the melting peak associated with α′-crystals will shift gradually to a higher temperature at longer t_c and merge with the melting peak located at 271°C eventually. Although an apparent single melting peak is detected for specimens crystallized at $T_c = 249–261$°C for short time, the half-height width of the peak is relatively large, suggesting the possible overlapping of the individual peaks associated with α′- and α″-forms. The overlapping of these two melting peaks makes the determination of true T_m uncertain and might result in a slight decrease of the apparent T_m measured as shown in Fig. 11. At T_c higher than 263°C, T_m' starts to increase with increasing T_c. Extrapolation of the T_m' versus T_c data for $T_c = 263–269$°C to the $T_m' = T_c$ value yields the values of T_m^0 and γ to be 281°C and 1.89, respectively. As mentioned previously, this value of thickening coefficient seems unreasonably large so that the linear *MX* plot is tentatively applied and given in Fig. 13 for several specified T_m^0. Fig. 14 shows the thickening coefficient at each specified T_m^0 derived from the slopes in Fig. 13. The determined T_m^0 for α-crystals is 294°C where the γ value is unity and the value of intercept, a, is 6.92. Similarly, the thickness of the virgin lamellae crystallized at T_c and the thickening coefficient can be derived as follows:

$$l^*(T_c) = \left(\frac{\sigma_e}{\Delta H_f}\right)_{\alpha\text{-form}}\left[\frac{1134}{294 - T_c} + 13.8\right] \quad (5)$$

$$\gamma(T_c, t_c) = \frac{M(t_c)}{X + 6.92} = \frac{567/(294 - T_m(t_c))}{567/(294 - T_c) + 6.92} \quad (6)$$

where $(\sigma_e/\Delta H_f)_{\alpha\text{-form}}$ is a parameter for α-form crystals and T_c is in the unit of °C. Eqs. (5) and (6) are valid for T_c ranged from 263 to 269°C for which a crystallization temperature dependence of T_m' is observed. The $\delta l^*/l^*$ fraction is about 0.29–0.23 which invalidates the assumption of linear HW plot method, i.e. $\delta l^*/l^* \sim 0$. On the other hand, the critical l^* remains more or less constant when specimens crystallized at T_c lower than 263°C since a constant zero crystallinity T_m' is observed (Fig. 12). The reason to cause the constant T_m' at 271°C for α-crystals crystallized at $T_c = 249–261$°C is uncertain at present. According to Eq. (6), the γ value is increased with increasing T_c (or t_c), being 1.04 at 263°C and 1.20 at 269°C at a given t_c of 60 min.

Fig. 15 shows the variation of l^* with T_c for both α- and β-crystals, as determined from Eqs. (3) and (5). In order to obtain the l^* value, the $\sigma_e/\Delta H_f$ values for α- and β-form crystals have to be known first. On studying the electron

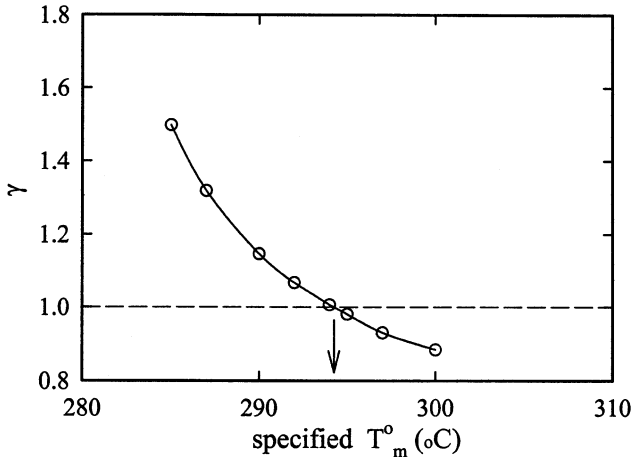

Fig. 14. Calculated thickening coefficients, γ, at different specified equilibrium melting temperatures, T_m^0, for α-form specimens (the genuine T_m^0 is determined at $\gamma = 1.0$ as pointed by the arrow).

diffraction of sPS solution-grown single β-crystals, Tosaka et al. [31] have measured the thickness of single lamellar crystals crystallized at various T_c. By plotting the l^* versus $1/\Delta T$ (Fig. 2 in Ref. [31]), the $(\sigma_e/\Delta H_f)_{\beta\text{-form}}$ value is deduced from the slope to be 0.2 nm, whereas the intercept gives δl^* to be about 3.47 nm, leading a $\delta l^*/l^*$ value about 0.35–0.58 which is consistent with our present results. When the derived $(\sigma_e/\Delta H_f)_{\beta\text{-form}}$ value is substituted into Eq. (3), the dependence of l^* on T_c for β-crystals is shown by the solid line in Fig. 15. The initial l^* is 4.3 nm at $T_c = 250$°C and is gradually increased to 5.7 nm at $T_c = 270$°C. A similar length scale of lamellar thickness is also obtained when transmission electron microscopy is conducted on the specimens after thin-sectioning and staining [17]. It is not an easy task, on the other hand, to obtain the $(\sigma_e/\Delta H_f)_{\alpha\text{-form}}$ value since the relation of l^* with $1/\Delta T$ for α-crystals is hardly obtained due to its less stability. There is no reported value in the literature at present. Recently, crystal transition from metastable phase to stable phase has been discussed based on the polymorphic nature of crystals. On studying the metastability and transition of PE hexagonal (h) crystals to PE orthorhombic (o) crystals, Keller et al. [29] have systematically discussed and compared the relative level of $\sigma_e/\Delta H_f$ in both crystals. Based on a theoretical consideration, it has been estimated that both σ_e and ΔH_f for the metastable h crystals are smaller than those for the stable o crystals, i.e. $(\sigma_e)_h \sim 1/7(\sigma_e)_o$ and $(\Delta H_f)_h \sim 1/2(\Delta H_f)_o$. In other words, a rough estimate of $(\sigma_e/\Delta H_f)_h/(\sigma_e/\Delta H_f)_o$ ratio is ca. 0.28–0.70 for PE, depending on the limited experimental data available. Since sPS possesses similar polymorphic behavior, e.g. stable β-form and less stable (or metastable) α-form [25], the relation $(\sigma_e/\Delta H_f)_{\alpha\text{-form}}/(\sigma_e/\Delta H_f)_{\beta\text{-form}} < 1.0$ is tentatively applied as a first approximation. For illustration purpose, the circle and square symbols in Fig. 15 are determined for α-crystals with a $(\sigma_e/\Delta H_f)_{\alpha\text{-form}}$ of 0.08 and 0.1 nm, respectively. It is evident that the l^* for α-crystals is relatively smaller than that for β-crystals, provided that $(\sigma_e/\Delta H_f)_{\alpha\text{-form}}/(\sigma_e/\Delta H_f)_{\beta\text{-form}}$ ratio is smaller than 0.4. Thus, formation of α-nuclei is much easier than β-crystals in the whole T_c range studied, suggesting by the size difference of the virgin lamella. Of course, a larger $(\sigma_e/\Delta H_f)_{\alpha\text{-form}}/(\sigma_e/\Delta H_f)_{\beta\text{-form}}$ ratio will lead to the inverse results, as shown in Fig. 15. In consideration of the metastable nature of α-crystals [25], it is unlikely for $(\sigma_e/\Delta H_f)_{\alpha\text{-form}}$ to be larger than 0.1 nm where there is no possibility for the α-crystals to develop earlier than β-crystals which is contrasted with experimental findings. More knowledge of the $(\sigma_e/\Delta H_f)_{\alpha\text{-form}}$ is required to conclude the trend proposed.

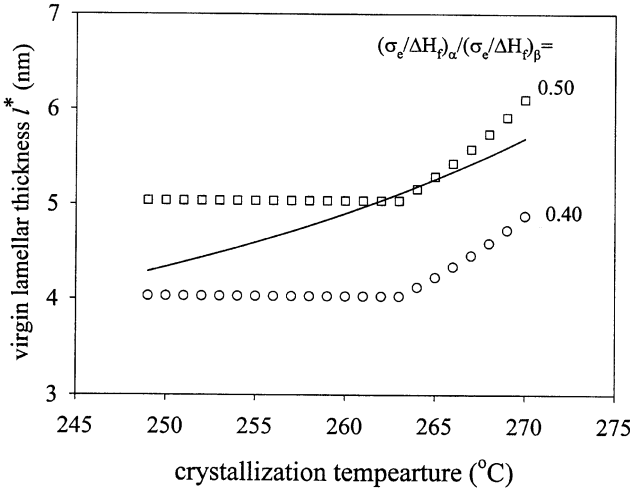

Fig. 15. Dependence of virgin lamellar thickness on the crystallization temperature (solid line for β-crystals with $\sigma_e/\Delta H_f = 0.2$ nm, circle symbols for α-crystals with $\sigma_e/\Delta H_f = 0.08$ nm, square symbols for α-crystals with $\sigma_e/\Delta H_f = 0.1$ nm).

3.4. Comparison of crystallization kinetics for α- and β-form crystals

According to Figs. 3 and 9, it takes longer time to initiate crystallization for specimens crystallized at higher T_c in both systems. One should be reminded that the usage of lower holding temperature (280°C instead of 300°C) for α-form specimens is to prevent the possible crystal transformation from α- to β-form found previously [3].

To further compare the crystallization evolution for both crystals, the melting behavior of neat specimens after crystallized at 255°C for varying lengths of time is shown in Fig. 16 and the measured enthalpies are plotted against t_c in Fig. 17. The melting peak in Fig. 16(a) is seen in the trace for 8 min of crystallization at 268.4°C, giving a melting enthalpy of 2.2 J/g. With increasing t_c, the melting peak moves up in temperature, reaching 269.5°C after 720 min of crystallization, involving an increase in melting enthalpy to 28.1 J/g. The behavior of α-form specimens in Fig. 16(b) is essentially similar to that of β-form specimens. The position of melting peak is increased from 270.2°C at

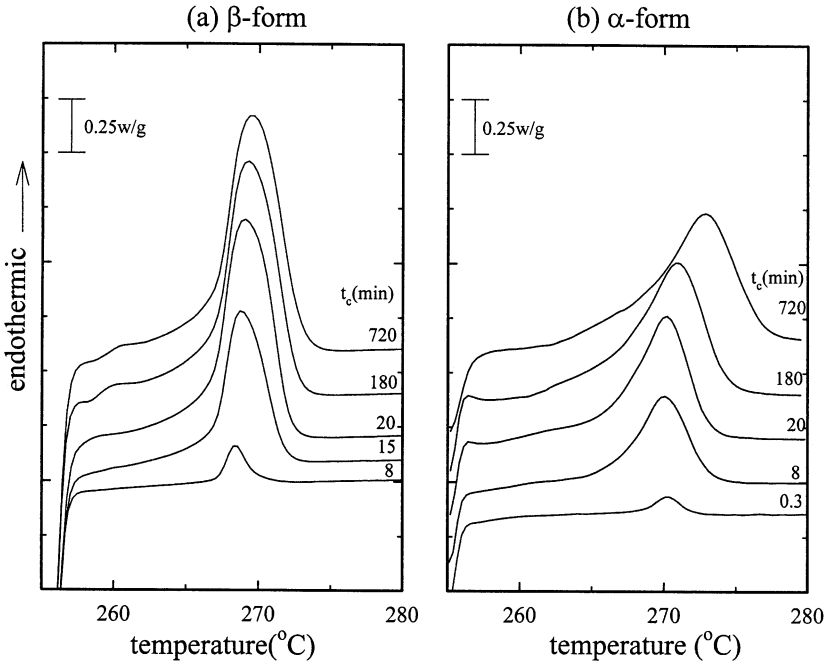

Fig. 16. Crystallization evolution of sPS specimens crystallized at 255°C: (a) β-form crystals, (b) α-form crystals.

$t_c = 0.3$ min to 272.8°C at $t_c = 720$ min, involving an increase in enthalpy from 1.3 to 21.3 J/g accordingly. After prolonged crystallization, however, a more broader distribution of lamellar thickness is found for α-crystals as revealed by a larger half-height width at $t_c = 720$ min, in comparison with β-crystals. Also given in Fig. 17 is the amount of accumulative enthalpy release (represented by the open square symbols) during isothermal crystallization of β-crystals obtained from the crystallization exotherm. Unfortunately, the corresponding crystallization exotherm for α-crystals at 255°C is absent due to the sensitivity limitation of DSC, resulting from the extremely short induction time, ca. 0.1 min shown in Fig. 17. For β-crystals, it is intriguing to note that similar crystallization kinetics are substantially obtained either from the exothermic crystallization process or from the endothermic melting process after crystallization. Based on this observation, it is suitable to use the melting enthalpy data for kinetic analyses at relatively high T_c where exothermic curves for isothermal crystallization are infeasible to obtain due to the practical limitation of DSC. As shown in Fig. 17, it seems that different crystalline entities and habits of crystallization are applied to both crystals. In contrast to β-crystals, α-form crystals possess a shorter induction time and a smaller melting enthalpy to the final extent. To reveal the crystallization details, the data are further presented in the form of Avrami plots and are shown in Fig. 18. The Avrami exponents determined from the slopes are 0.7 and 2.7 for α- and β-form crystals, respectively. This leads us to conclude that different nucleation mechanisms and nuclei entities are developed for both crystallization evolutions. Based on the Avrami exponents obtained, athermal nucleation process with fibrillar crystals and spherulitic crystals are expected in α- and β-form specimens, respectively. Due to the one-dimensional growth for α-crystals, the crystallization time required to reach the final extent is much longer than that for β-crystals where three-dimensional crystal growth takes place if the nucleation density is similar. Indeed, it takes 37.3 min for α-crystals to reach 90% relatively crystallinity in comparison with 13.5 min for β-crystals although the crystallization half time for α-crystals is smaller, being 6.7 min compared to 8.7 min for β ones. On the study of cold crystallization of sPS from amorphous state, Woo et al. [32,33] have obtained an Avrami exponent

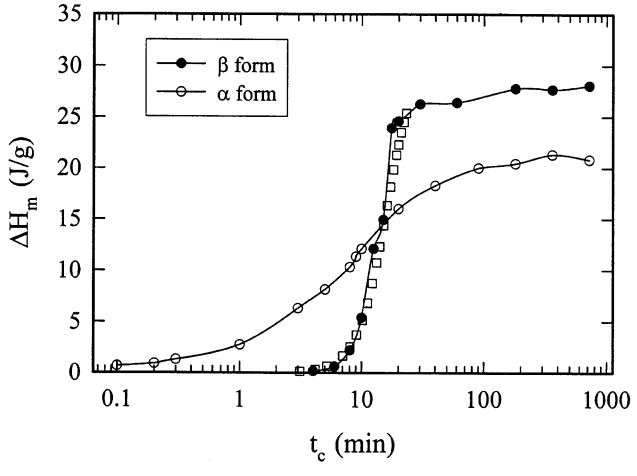

Fig. 17. Crystallization evolution for α- and β-form crystals crystallized at 255°C (circle symbols are obtained from endothermic melting during heating scans (Fig. 16) and square symbols are obtained from the crystallization exotherm).

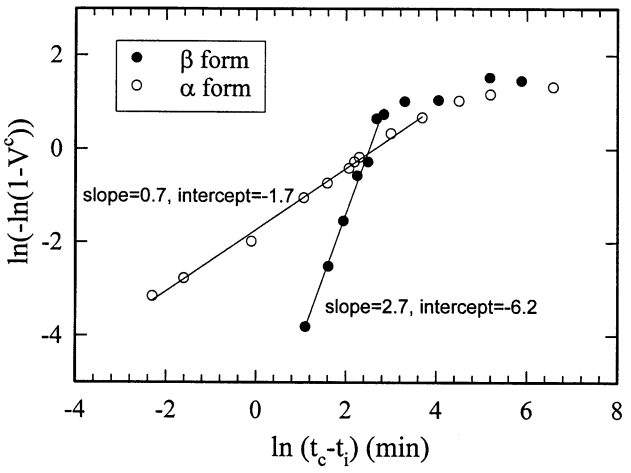

Fig. 18. Avrami plots for α- and β-form specimens crystallized at 255°C (t_i is the induction time).

about 2.4 for α-form specimens (most likely α′-form crystals according to their WAXD patterns in Ref. [32]). This is in contrast with our results for α″-crystals as shown in Fig. 1 and might suggest further that α′- and α″-form crystals exhibit different crystallization habits.

3.5. Crystal development for specimens with mixed α/β-form

It has been pointed out [18,19,30] that three endothermic melting peaks are normally observed during DSC scans for specimens with mixed α- and β-crystals crystallized at low temperatures (below 247°C) prior to heating. On the other hand, only one melting peak appears when T_c is high enough (above 251°C). In an attempt to reveal the crystallization evolution for specimens with mixed α/β-crystals, the melting endotherm obtained for as-received sPS pellets after being crystallized at 240°C for $t_c = 4$ min is shown in Fig. 19. Three melting peaks positioned at 260.3, 263.7 and 270.1°C are evident. The melting enthalpy is 26.2 J/g. For comparison purpose, the corresponding endotherms for neat α- and β-form crystals are included in Fig. 19 as well. Only two melting peaks are detected at 266.6 and 271.7°C for specimens with neat α-crystals. In addition, melting enthalpy is reduced to a lower value of 18.8 J/g, suggesting a lower level of crystallinity developed in the α-form specimens. Regarding the specimens with neat β-crystals, the melting enthalpy is 26.3 J/g and double-melting behavior is also observed with the melting peaks located at 260.3 and 270.8°C, which are, respectively, close to the lowest and highest melting peaks of mixed-form specimens. Thus, for mixed form sPS, we can expect that the lowest melting peak is related to the melting of β-crystals and the highest melting peaks are associated with melting of both α- and β-crystals in consideration of the relative peak positions. The intermediate melting peak should be relevant to the melting of α-crystals, as pointed out previously [12,18]. However, a 2.9°C difference (263.7 versus 266.6°C) in the peak position is evident, when compared to the neat α-form specimens. It suggests that melting-recrystallization mechanism of β-crystals has to be taken into account for which the recrystallization exotherm will shift the melting peak of α-crystals to a lower temperature as observed. Thus, the intermediate melting peak is superposition of two contributions; one is the endotherm associated with melting of α-crystals developed prior to the DSC scan, the other is the exotherm corresponds to recrystallization of β-crystals following its melting at 260.3°C. As a matter of fact, the position of the intermediate melting peak depends on the relative resultant level of β-form recrystallization exotherm and α-form melting endotherm. Therefore, the intermediate temperature should not readily be taken as the melting temperature of the α-crystals unless separation of the individual thermographs is carried out.

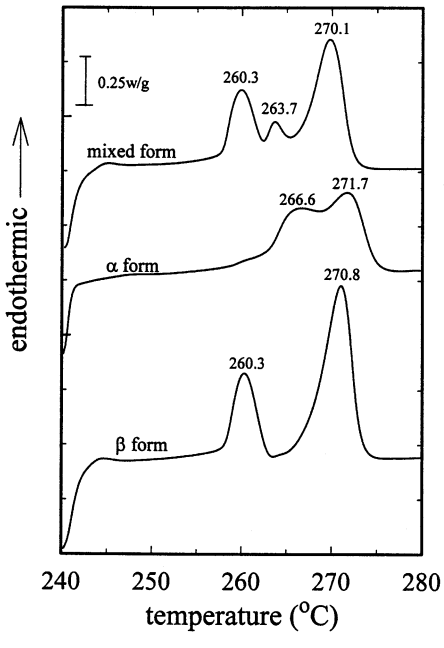

Fig. 19. Melting endotherms of sPS specimens (neat α, neat β and mixed α/β-form) crystallized at 240°C for 4 min.

To further explore the crystallization evolution for α- and β-form specimens at $T_c = 240$°C, the melting endotherms at several specified t_c are shown in Fig. 20. For specimens with α-form crystals crystallized for $t_c = 0.1$ min, two melting peaks located at 265.9 and 271.4°C are readily observed. It has been suggested [30] that the high-melting peak is related to the ordered α″-form and the low-melting peak is associated with the less ordered α′-form. The high-melting peak temperature is maintained at about 271°C while the low-melting peak temperature increases gradually to 268.7°C at $t_c = 720$ min where an asymmetric melting peak is formed due to the peak overlapping. Thus, thickening for the α′-form crystals is more pronounced than that for α″-form crystals. Moreover, the height of the high-melting peak remains unchanged, whereas that of the low-melting peak increases with t_c, indicating the slow population increase of

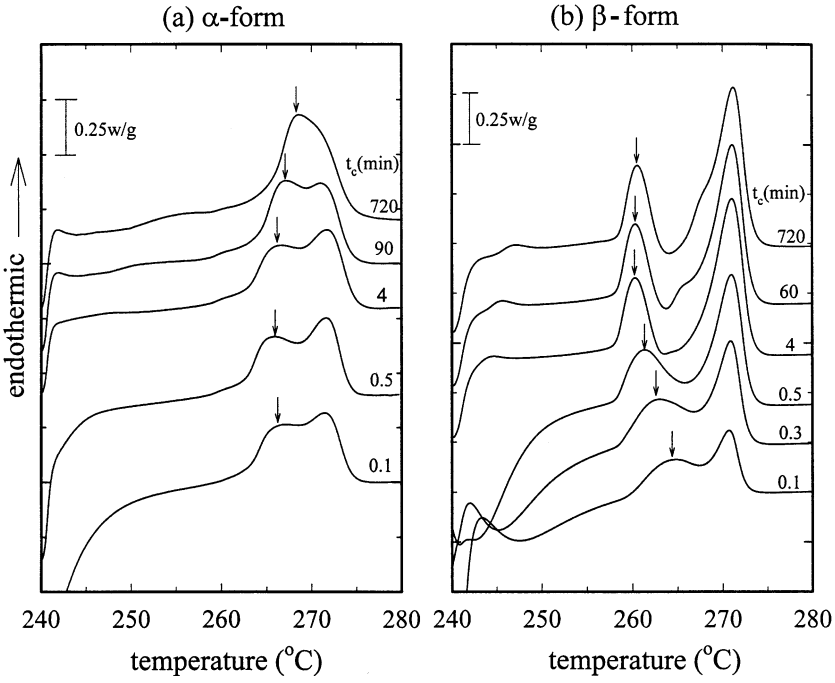

Fig. 20. Crystallization evolution of sPS specimens crystallized at 240°C: (a) α-form crystals, (b) β-form crystals (the arrows pointing movement of the low-melting peak).

the less ordered α'-form crystals but leaving the content of ordered α''-form crystals intact.

For specimens with β-form crystals, two melting peaks are readily detected at 264.8 and 270.7°C for crystallization $t_c = 0.1$ min, showing a feature reminiscent of that for α-form although the peak positions are slightly different. In contrast to that for α'-crystals, however, the low-melting peak gradually shifts to a lower temperature (260.3°C at $t_c = 4$ min) and remains unchanged until $t_c = 720$ min. Thus, either lamellar thinning or crystal transformation takes place during the very early period ($t_c = 0.1$–4 min). The position of high-melting peak at 270.7°C, on the other hand, is essentially independent of crystallization time (that is similar with the high-melting peak for α-form crystals) but its height increases with increasing t_c which is different from that for α''-crystals. Reproducibility of Fig. 20(b) has been confirmed, especially for $t_c = 0.1$–4 min. The movement of the low-melting peak to low temperatures is of great significance in consideration of the possible crystal transformation from α'- to β'-form due to the stability inversion with lamellar thickness, as suggested recently by Ho et al. [25].

4. Conclusions

When crystallized from melt, sPS can occur in two crystalline forms, denoted as α- and β-form crystals. The α- and β-form crystals of sPS constitute a unique pair crystalline structures which display complicated habits of crystallization and melting behavior. The orthorhombic β-form is more stable than the hexagonal α-form. Hence, not only the crystal form itself but also the crystal transformation (α to β) and possible recrystallization during melting have been observed, leading to the determination of thermodynamic parameters for individual crystals infeasible for specimens with mixed α/β-crystals. Thus, the first aim of this study is to prepare sPS specimens with neat α-form (and β-form) crystals through hot press molding for further characterization of each crystal form. Results show that neat α''-crystals can be obtained when the as-received pellets are molded at low temperature (260°C) and high pressure (15.5 MPa); whereas neat β'-crystals are favored when molded at high temperature (290°C) and low pressures (0.6 MPa). The crystal structures of the as-molded specimens were verified through WAXD and FTIR techniques.

The equilibrium melting temperature of crystalline polymer is a quantity which is of eminent importance in determining the crystallization behavior of the polymer. In an effort to obtain equilibrium melting temperatures for α- and β-form sPS, attention was directed to the extrapolative method involving the dependence of the observed melting temperatures on the crystallization temperature and time. A low level of crystallinity is desirable in order to minimize any isothermal thickening due to prolonged crystallization, leading to the variation of thickening coefficient. The equilibrium melting temperatures deduced from the linear HW plot of melting temperature at zero crystallinity against crystallization temperature were found to be 281 and 291°C for α- and β-form crystals, respectively. In addition, a

recently developed linear *MX* plot (modified non-linear HW plot) was also carried out and larger equilibrium melting temperatures were obtained, ca. 294 and 320°C for α- and β-form crystals, respectively. Based on this new approach, the temperature dependence of initial lamellar thickness for α- and β-nucleus is estimated and compared with each other as a function of T_c.

When specimens with mixed-form crystals are crystallized isothermally at 240°C, three melting peaks are observed on the subsequent DSC heating scans. Compared to the corresponding endotherms for neat α- and β-form specimens, it is concluded that the lowest melting peak is related to β-crystals, the intermediate melting peak is associated with α-crystals and the highest melting peak is relevant with both α- and β-crystals.

Acknowledgements

Support from National Science Council of Republic of China through a grant (NSC89-2216-E-006-050) is gratefully acknowledged. We also thank Prof. F.-C. Chiu at CGU for helpful discussions.

References

[1] Rosa CD, Guerra G, Petraccone V, Corradini P. Polym J 1991;23:1435.
[2] Rosa CD, Rapacciuolo M, Guerra G, Petraccone V, Corradini P. Polymer 1992;33:1423.
[3] Guerra G, Vitagliano VM, Rosa CD, Petraccone V, Corradina P. Macromolecules 1990;23:1539.
[4] Rastogi S, Goossens JGP, Lemstra PJ. Macromolecules 1998;31:2983.
[5] Candia FD, Carotenuto M, Guadagno L, Vittoria V. J Macromol Sci, Phys 1996;B35:265.
[6] Immirzi A, Candia FD, Iannelli P, Zambelli A, Vittoria V. Makromol Chem, Rapid Commun 1988;9:761.
[7] Chatani Y, Shimane Y, Inoue Y, Inagaki T, Ijitsu T, Yukinari T. Polymer 1992;33:488.
[8] Guerra G, Musto P, Karasz FE, MacKnight WJ. Makromol Chem 1990;191:2111.
[9] Zimba CG, Rabolt JF, English AD. Macromolecules 1989;22:2867.
[10] Cimmino S, Pace ED, Martuscelli E, Silvestre C. Polymer 1991;32:1080.
[11] Arnauts J, Berghmans H. Polym Commun 1990;31:343.
[12] Woo EM, Wu FS. Macromol Chem Phys 1998;199:2041.
[13] Gvozdic NV, Meier DJ. Polym Commun 1991;32:493.
[14] Albrecht T, Strobl G. Macromolecules 1996;29:783.
[15] Sun Z, Morgan RJ, Lewis DN. Polymer 1992;33:660.
[16] Varga J. J Mater Sci 1992;27:2557.
[17] Hsu YC. Master Thesis. Taoyuan, Taiwan: Yuan-Ze University; 1999.
[18] Hong BK, Jo WH, Lee SC, Kim J. Polymer 1998;39:1793.
[19] Chen CC. Master Thesis. Taoyuan, Taiwan: Yuan-Ze University; 1999.
[20] Musto P, Tavone S, Guerra G, Rosa CD. J Polym Sci, Polym Phys 1997;35:1055.
[21] Gianotti G, Valvassori A. Polymer 1990;31:473.
[22] Paszlor JR, Landes BG, Karjala PJ. Thermochim Acta 1991;177:187.
[23] Bark M, Zachmann HG, Alamo R, Mandelkern L. Makromol Chem 1992;193:2363.
[24] Xu J, Sriniva S, Marand H, Agarwal P. Macromolecules 1998;31:8230.
[25] Ho RM, Lin CP, Tsai HY, Woo EM. Macromolecules 2000;33:6517.
[26] Alamo RG, Chan EKM, Mandelkern L, Voigt-Martin IG. Macromolecules 1992;25:6381.
[27] Marand H, Xu J, Srinivas S. Macromolecules 1998;31:8219.
[28] Lauritzen Jr JI, Hoffman JD. J Appl Phys 1973;44:4340.
[29] Keller A, Hikosaka M, Rastogi S, Toda A, Barham PJ, Goldbeck-Wood G. J Mater Sci 1994;29:2579.
[30] Lin RH, Woo EM. Polymer 2000;41:121.
[31] Tosaka M, Hamada N, Tsuji M, Kohjiya S. Macromolecules 1997;30:6592.
[32] Woo EM, Sun YS, Lee ML. Polymer 1999;40:4425.
[33] Wu FU, Woo EM. Polym Engng Sci 1999;39:825.